Salt-induced liquid-liquid phase separation of protein-surfactant complexes

Janaky Narayanan* and Vinod W. Deotare
Department of Physics, R. J. College, Ghatkopar (West), Mumbai 400 086, India
(Received 27 August 1998; revised manuscript received 2 June 1999)

We report the cloud-point curve determination of lysozyme-sodium-doderyl-sulfate (SDS) complexes in solution. By varying the *p*H, salt concentration, and relative ratio of lysozyme to SDS, the phenomenon of clouding and liquid-liquid phase separation is investigated under different solution conditions. For the temperature, concentration, and *p*H ranges used in this study, the clouding phenomenon appears to be controlled by the electrostatic interaction between the lysozyme-SDS complexes. Any change in the solution condition that leads to a decrease in the charge on the lysozyme-SDS complexes results in an increase in cloud-point temperature. A generalized Flory-Huggins theory for polydisperse polymers is used to describe the cloud-point curve. [S1063-651X(99)06410-7]

PACS number(s): 87.15.Nn, 64.10.+h, 64.70.Ja, 64.75.+g

INTRODUCTION

The interactions and structure of complexes formed by proteins with surfactants in aqueous solutions have been studied extensively [1–12]. Anionic surfactants such as sodium dodecyl sulfate (SDS) interact strongly with oppositely charged globular proteins and denature them. The unfolding of the proteins by SDS is considered to be caused by binding of the SDS molecules to the hydrophobic portion of the polypeptide chain. The binding of SDS to proteins is studied by determining the binding isotherms in which the number of surfactant molecules bound per protein molecule ($\overline{\nu}$) is plotted as a function of surfactant concentration [13]. At low surfactant concentration this number increases slowly, characterizing a specific and noncooperative binding, followed by a rapid increase due to nonspecific and cooperative binding. The unfolding of the proteins is believed to occur in the cooperative binding region. Further increase in surfactant concentration leads to a saturation region where further binding of the surfactant does not occur on the protein and normal micelle formation occurs as excess surfactant is added.

The microstructure of protein-surfactant complexes has been investigated by various techniques [3–11]. The structure of bovine serum albumin (BSA) and ovalbumin (OVA) complexes with SDS and lithium dodecyl sulfate (LDS) was described in terms of a necklace model by using a small angle neutron scattering (SANS) study [3–5]. This model assumed that denatured polypeptide chains were flexible in solution and micellelike clusters of SDS/LDS were formed around the hydrophobic patches of the protein backbone along the unfolded polypeptide chain. Investigations of the BSA-SDS system by spectroscopic probe techniques—steady state and time-resolved fluorescence, electron spin resonance, and deuterium NMR spectroscopy—led to the conclusion that the structure of the complexes was of the necklace and bead type in which unfolded protein wrapped around surfactant micelles [8]. The wrapping of protein around the micelles decreases the mobility of the head group and presumably lowers the electrostatic field. The first cloud-point curve determination of BSA-SDS complexes in solution was done by Guo and Chen [14] and they described the cloud-point curve using generalized Flory-Huggins theory, assuming the structure of the complexes to be polymerlike.

In this paper we investigate the protein, lysozyme, which is a widely studied globular protein [15,16]. Its molecular weight is 14 600 and the isoelectric point (*pI*) is 11.0. Hence it is positively charged in aqueous solutions. Its native conformation is a prolate ellipsoid with dimensions $45\times30\times30$ Å. The phase equilibrium of lysozyme and SDS in water have been investigated recently by Moren and Khan [12] over a wide concentration range of 20 wt % protein and 20 wt % surfactant. The phase diagram was discussed in terms of electrostatic and hydrophobic effects elucidating the protein-surfactant interactions. Liquid-liquid and solid-liquid phase separation of aqueous solutions of lysozyme induced by a series of chloride, bromide, and sulfate salts have been investigated by Broide, Tominc, and Saxowsky [17]. The phase-separation temperature was found to be very sensitive to the identities of both the cation and anion of the added salt. While modeling the protein interactions, they found that the Derjaguin-Landau-Verwey-Overbeek (DLVO) theory [18] for the interaction energy between charged spheres could not account for their observations and hydration forces play an important role in protein interactions.

In this paper, we report the cloud-point curve determination of lysozyme-SDS complexes in solution along the guidelines given by Guo and Chen [14] for the BSA-SDS system. It is found that when the *p*H of the solution is close to the *pI* of the protein and the ionic strength of the solution is sufficiently high, liquid-liquid phase separation occurs as the solution of lysozyme-SDS in proper weight ratio is cooled below its cloud-point temperature. The solution gets cloudy and separates into two coexisting liquid phases, one rich in protein and the other poor in protein. The cloud-point temperature is found to be very sensitive to the ionic strength, *p*H, and relative proportion of lysozyme and SDS. Also, as observed by Moren and Khan [12], on heating to 55 °C or above and cooling, the samples give rise to heat-set gels, especially for large weight percent. This sets a limit to the concentration range that can be explored. The cloud-

*Author to whom correspondence should be addressed. Electronic address: narayan@bom2.vsnl.net.in

point curve is explained using generalized Flory-Huggins theory for polydisperse polymers [14,19,20]. However, the interplay of the various interactions that leads to the clouding phenomenon seems to be too elusive to be accounted for quantitatively.

MATERIALS AND METHODS

Lysozyme from chicken egg whites (L6876) was bought from Sigma Chemicals (lot 57H7045) and used without further purification. SDS purchased from Loba Chemie (biochemical grade) and sodium chloride (NaCl) from Merck were used as received. Carbonate buffer solutions of pH $=9.7$, 10.0, and 10.2 were prepared using $0.025M$ $NaHCO_3$ and $0.025M$ Na_2CO_3 by adjusting their relative proportions. Samples were prepared by dissolving weighed quantities of lysozyme, SDS, and NaCl individually in buffer and then mixing them in the order lysozyme plus SDS plus NaCl. For convenience, a 15 wt % SDS stock solution in buffer was used in the preparation of samples. Lysozyme is soluble in aqueous solutions with pH$=10$, but the solution is slightly turbid, indicating some aggregation [21]. However, on addition of SDS solution and mixing thoroughly it becomes clear. Later, NaCl solution was added and the sample was stirred with a magnetic stirrer. After mixing, the solution was left undisturbed for another 2 h so that the complex reached equilibrium.

For the cloud-point determination, the solution was poured into a 1 cm diameter glass vial having an airtight cap to prevent evaporation. The sample vial was placed in the thermostat bath of Brookhaven BI-90 particle sizer, employing a He-Ne laser ($\lambda = 632.8$ nm). The scattering angle was 90°. The sample was heated to a temperature above the cloud point until the solution became clear. Then the temperature was successively reduced by one or two degrees and the sample was equilibrated for 5 min at each temperature. The count rate, which is a measure of the scattered intensity, was monitored for 5 min at each set temperature and the average value was recorded. A plot of count rate vs temperature shows a sharp change of slope at the cloud-point temperature (Fig. 1).

In order to settle the ambiguity in selecting the linear regimes in the high temperature and low temperature part of the curve, the following method was adopted. The data were split into two groups with varying number of points in each group. Both the groups were fitted by linear regression and the average value of the correlation coefficient (r_{av}) was noted down. The maximum of the r_{av} would correspond to that grouping of the data which would have the best linear fit on both low and high temperature regimes. The cloud point was determined by grouping the data as per this r_{av} value.

The cloud-point temperature has been found by solely cooling the sample. In order to eliminate the error of undercooling the sample to induce phase transition as is mentioned in Ref. [17], the experiment was repeated by heating the same sample and measuring the count rate at the same temperatures as were set while cooling. For low concentration samples, the cloud-point temperature measured by heating the sample was found to be 1 °C to 2 °C higher than that found by cooling the sample. For samples of high concentration, the fluctuations in count rate while reheating the sample were too large to find a meaningful average.

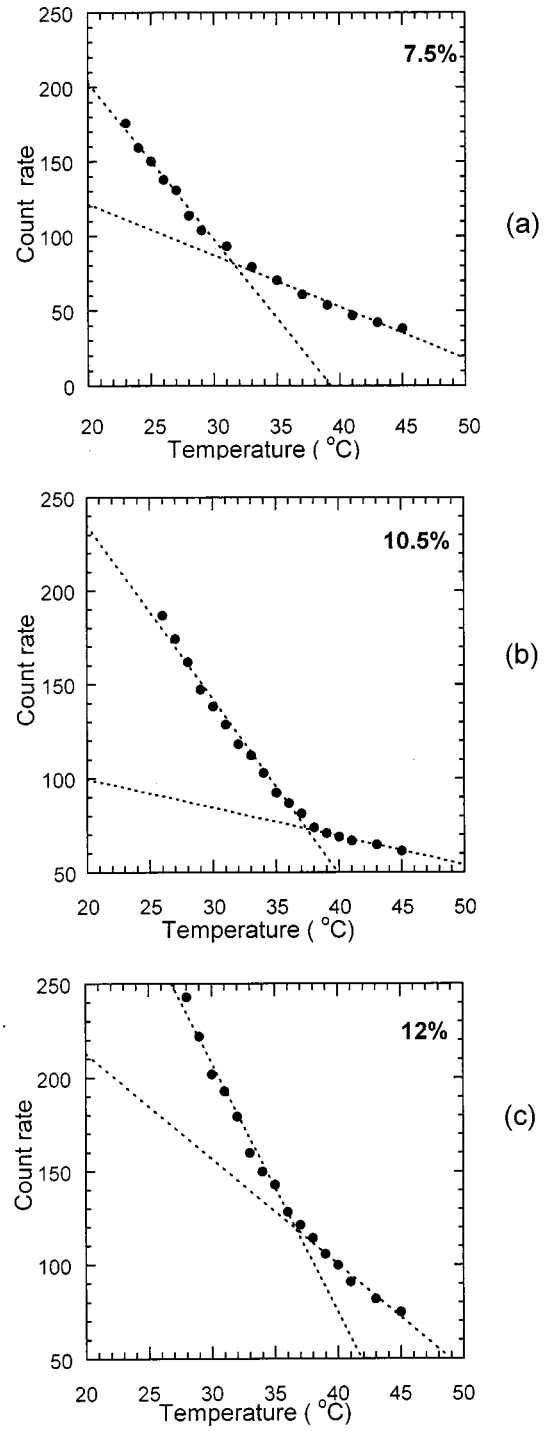

FIG. 1. Plot of count rate vs temperature for lysozyme plus SDS of total weight percent, (a) 7.5%, (b) 10.5%, and (c) 12%. Lysozyme:SDS=1:2, pH$=10$, and NaCl concentration is equal to $0.4M$. The cloud-point temperature is at the point of intersection of the straight line fits to the high and low temperature regions of the graph.

The temperature range used in this study was 20–50 °C. At temperatures less than 20 °C there is condensation of water vapor around the sample vial. Since there is no purging gas facility in the instrument, only those concentrations which would have cloud-point temperature greater than 25 °C were chosen for this study.

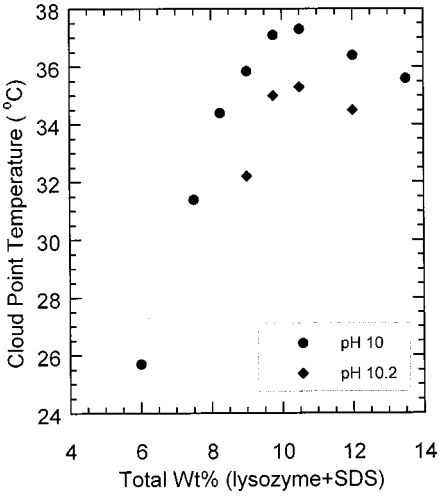

FIG. 2. Cloud-point curve for lysozyme-SDS complexes in buffer solutions of *p*H 10 and 10.2 in the presence of 0.4*M* NaCl. The weight ratio of lysozyme:SDS=1:2.

Samples of low concentration phase separated very slowly below the cloud point. At higher concentrations, the phase separation was faster (within a day or two) with the lower phase appearing more dense and turbid than the upper phase. On reheating the phase-separated sample above the cloud-point temperature, both phases cleared but maintained a meniscus at the boundary of the two phases. The sample could later be homogenized by shaking to get a visually clear one phase. In low concentration samples, the data corresponding to cloud-point measurements were reproducible by heating and cooling the same sample two or three times. However, for high concentrations, especially beyond the critical point, the reproducibility of the results was limited due to formation of gel on repeated heating. Hence verification of the results had to be done by preparing fresh samples of the same concentration.

The presence of protein in both phases of fully phase-separated samples was confirmed as follows.

A solution of total weight percent of 0.6% with lysozyme-:SDS in the weight ratio of 1:2 was prepared in buffer of *p*H 10 in the presence of 0.4*M* NaCl. This was diluted with buffer to get a standard solution with protein concentration of 16 mg per 100 ml. Protein estimation was done by the method of Lowry *et al.* [22]. The absorbance of the sample was measured using a Jasco V-530 UV/VIS Spectrophotometer and a calibration graph of absorbance vs protein concentration was determined. From the upper phase of a fully phase-separated sample of total weight percent of 12% with lysozyme:SDS in the weight ratio 1:2 in buffer of *p*H 10 in the presence of 0.4*M* NaCl, 0.1 ml of the solution was drawn out carefully and diluted by 50 times. The absorbance of this sample was measured and from the calibration graph, the protein concentration in the upper phase was determined. For this sample, protein was found to phase separate in the ratio 1:17 by weight in the upper and lower phases at room temperature. The presence of protein in the upper phase was also confirmed for fully phase-separated samples of total weight percent of 9 and 7.5.

RESULTS

The cloud-point curve determined for lysozyme-SDS complexes in buffer solutions of *p*H=10 in the presence of 0.4*M* NaCl is shown in Fig. 2. The weight ratio of lysozyme to SDS was maintained at 1:2. The total weight percent of lysozyme plus SDS in the solution was varied from 6% to 13.5%. For comparison, we have also plotted the data on measurements at *p*H=10.2.

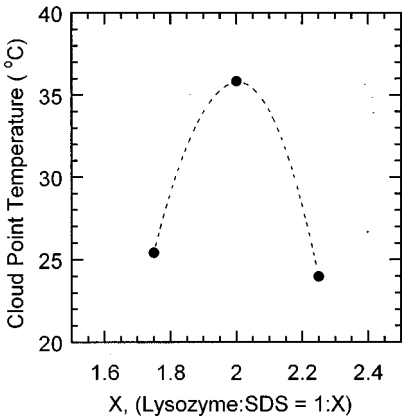

FIG. 3. Variation of cloud-point temperature with SDS concentration. Lysozyme concentration is equal to 3 wt %, NaCl concentration is equal to 0.4*M*, *p*H=10. The dotted line is a guide to the eye.

The effect of SDS concentration on cloud-point temperature was studied by fixing the lysozyme concentration at 3 wt %, salt concentration at 0.4*M*, and varying the SDS concentration for different weight ratios of lysozyme to SDS. The samples were prepared in a buffer of *p*H=10. It was found that for weight ratios of 1:1.5 and 1:2.5 of lysozyme-:SDS, the solution did not show any clouding when cooled up to 20 °C. For intermediate weight ratios, the clouding was observed with cloud-point temperature passing through a maximum at 1:2 (Fig. 3).

The effect of *p*H on cloud-point temperature is shown in Fig. 4. The total weight percent of lysozyme plus SDS was maintained at 9 wt % with lysozyme:SDS in the weight ratio of 1:2. The salt concentration was kept at 0.4*M*. The samples were prepared in buffers of *p*H 9.7, 10.0, and 10.2. The cloud-point temperature was found to pass through a maximum at *p*H~10.0.

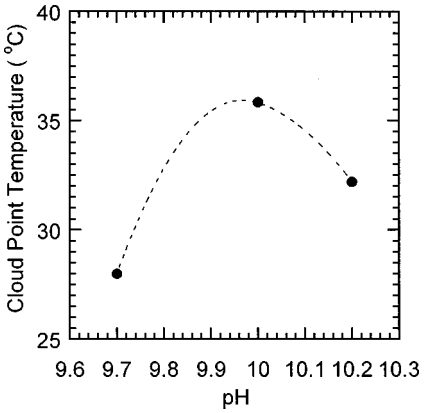

FIG. 4. Variation of cloud-point temperature with *p*H. Total weight percent of lysozyme plus SDS is equal to 9 wt %, lysozyme-:SDS weight ratio is equal to 1:2, NaCl concentration is equal to 0.4*M*. The dotted line is a guide to the eye.

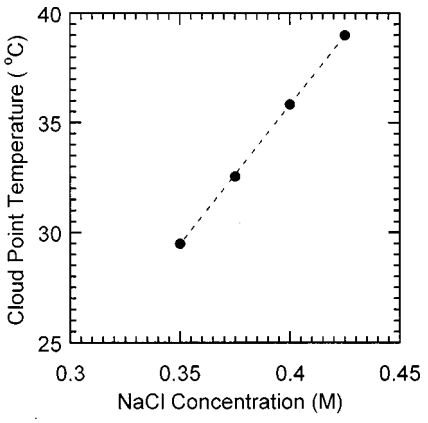

FIG. 5. Variation of cloud-point temperature with NaCl concentration. Total weight percent of lysozyme plus SDS is equal to 9 wt %, lysozyme:SDS weight ratio is equal to 1:2, pH=10. The dotted line is a guide to the eye.

The effect of salt on cloud-point temperature was studied by fixing the total weight percent of lysozyme plus SDS at 9% in buffer of pH=10.0 (lysozyme:SDS=1:2) and varying the salt concentration from 0.3M to 0.45M. For 0.3M salt, the solution remained clear at room temperature. As the salt concentration was increased from 0.35M to 0.425M, the cloud-point temperature also increased (Fig. 5). A sample with 0.45M salt was not clear up to 55 °C. On heating to 60 °C it cleared, but on cooling there was irreversible phase separation with a formation of a gel that had a spongy texture. It has to be mentioned here that the pH of the solution changes on addition of salt, especially in large quantities [17,23]. Since lysozyme precipitates out in the presence of salt at this pH, we could not adjust the buffer solution pH in the presence of salt to required values and use it for dissolving lysozyme and SDS. Hence the pH values reported here are those of the buffer solutions used to dissolve lysozyme, SDS, and NaCl individually and then mix them in the same order. It was found that for the buffer solutions of pH =9.7, 10.0, and 10.2 used in this study, the relative decrement of pH in the presence of 0.4M salt was the same.

DISCUSSION

For a system exhibiting an upper consolute boundary, cooling below the cloud-point temperature produces a phase separation, which is driven by a net attraction between the molecules. The stronger the attraction, the higher is the cloud-point temperature. We find that the cloud-point temperature of lysozyme-SDS complexes is very sensitive to the ionic strength, pH, and relative proportion of lysozyme and SDS. This indicates that the screening of the electrostatic interaction plays an important role in deciding the net attractive force responsible for clouding.

The charge on lysozyme is $+7e$ at pH=9 and decreases rapidly as the isoelectric point at pH=11 is approached [15]. As mentioned earlier, the solution of lysozyme dissolved in buffers of pH$\approx$10 is turbid, indicating some aggregation. However, when SDS solution is added in the weight ratio of lysozyme:SDS=1:2, the solution clarifies. Moren and Khan [12] have determined the phase diagram for the lysozyme-SDS-water system. They found that addition of small amounts of SDS to an aqueous lysozyme resulted in precipitation. The yield of the precipitate increased as the number of SDS molecules per protein molecule (N_{SDS}/N_P) increased and reached a maximum at $N_{\mathrm{SDS}}/N_P=8$. This is attributed to complete charge neutralization of protein since at pH=7 the charge on lysozyme is $+8e$. On addition of more SDS, a complete redissolution of the precipitate occurred at about 19 SDS molecules per protein. For higher SDS concentration, a clear isotropic single solution phase was obtained. Hence the interaction between protein and surfactant for N_{SDS}/N_P >19 must be due to nonspecific and cooperative binding.

The lysozyme-SDS weight ratios of 1:1.75, 1:2, and 1:2.25 used in this study correspond to $N_{\mathrm{SDS}}/N_P=88$, 101, and 114, respectively. Hence it may be expected that SDS aggregates into micelles which get bound to the protein unfolding it. A rough estimate of the hydrodynamic radius of the lysozyme-SDS (1:2) complexes at 45 °C, pH=10, and [NaCl]=0.4M, determined from the count rate of the scattered light, was 150 Å, which is almost an order of magnitude higher than the mean radius of the protein.

The aggregation number of SDS micelles in water is 60 for a concentration of 69 mM ($\sim$2 wt %) which increases to about 1000 in the presence of 0.6M NaCl [24]. However, the micellelike aggregates formed on protein were found to be smaller than the corresponding micelles formed in protein-free solutions [3,8]. Guo and Chen [14] report that there is no substantial change observed in the cloud-point curve for SDS to BSA weight ratio varying between 2.2/1 and 3.2/1 except that the shape of the cloud-point curve becomes slightly flatter with increasing SDS to protein weight ratio. For these weight ratios N_{SDS}/N_P varies from 504 to 733. This suggests that these SDS concentrations are in the saturation binding region of the binding isotherm where free micelles may coexist with protein-bound micelles as the saturation binding of SDS to BSA is 1.4 g of SDS/g of protein [1,25].

For the lysozyme-SDS system, Fukushima *et al.* [9,10] have determined the binding isotherm at different pH and in the presence of salt. Beyond $\bar{\nu}=10$, the binding of SDS to lysozyme was found to be cooperative and $\bar{\nu}$ increased to as high as 70 in the cooperative binding region for salt concentrations ranging from 10 to 100 mM. Also the degree of counterion (Na^+) binding in the lysozyme-SDS complex was found to increase with $\bar{\nu}$ and approach the value of 0.7 for free SDS micelles for large values of $\bar{\nu}(\bar{\nu}>60)$. In Fig. 3 we observe that in the lysozyme-SDS system, the cloud-point temperature is highly sensitive to the relative weight ratio of lysozyme to SDS unlike the case of the BSA-SDS system [14]. For the lysozyme:SDS weight ratios of 1:1.75, 1:2, and 1:2.25, $N_{\mathrm{SDS}}/N_P=88$, 101, and 114, respectively, which are far less than those in the BSA-SDS system studied by Guo and Chen [14]. One possible explanation of the observed result could be that the SDS concentrations used in this study are in the cooperative binding region of the binding isotherm where no free micelles exist in the solution. The negatively charged SDS micellar aggregates bound to the protein may change the net charge of the lysozyme-SDS complex from a net positive to a net negative charge as the protein to surfactant ratio decreases. Increase in charge of either sign would increase the repulsive energy between the complexes, resulting in a lowering of cloud-point temperature.

Keeping the *p*H and salt concentration constant, if the charge on the protein can be tuned by changing the relative proportion of protein to SDS, then, by keeping the relative proportion of protein to SDS and the salt concentration constant, it should be possible to vary the charge on the lysozyme-SDS complexes by changing the *p*H of the solution. Since *pI* of lysozyme is 11.0, the charge on the protein progressively becomes more positive as *p*H is decreased below 11.0. If the negative charge on the SDS micellar aggregates bound to the protein remains the same at constant SDS concentration, the charge on the lysozyme-SDS complex can be changed by varying the *p*H. In Fig. 4, we find that the cloud-point temperature is very sensitive to *p*H and the effect of increasing *p*H at constant SDS concentration is the same as increasing SDS concentration at constant *p*H (Fig. 3).

That the charge on the protein-surfactant complex plays an important role in deciding the cloud-point temperature is demonstrated by Fig. 5, in which the cloud-point temperature is plotted against salt (NaCl) concentration, keeping the protein to surfactant weight ratio and the *p*H of the solution constant. As the salt concentration is increased, the cloud-point temperature increases monotonously till an irreversible phase separation occurs. The range of the repulsive Coulomb energy is decided by the Debye screening length κ^{-1}. At room temperature, $\kappa^{-1} \sim 3\,\text{Å}/\sqrt{I}$ where I is the ionic strength of the solution. In addition to the salt concentration, the counterion concentration also contributes to the ionic strength. The ionic strength due to counterions is given by $0.5\alpha(C\text{-CMC})$ [26] where α is the fractional charge on the SDS micelles, C is the molar concentration of SDS, and CMC is its critical micelle concentration. However, for SDS concentrations used in this study ($C \leqslant 9$ wt %, i.e., $\leqslant 0.32M$), since $\alpha \approx 0.3$ [10,27], the ionic strength due to counterions is negligible and hence $I \approx [\text{NaCl}]$. Increasing the ionic strength of the solution decreases the repulsive part of the interaction energy between the particles, which would increase the cloud-point temperature as seen in Fig. 5. Thus the ionic strength seems to play an important role in the liquid-liquid phase separation. This is supported by the recent finding of Sato *et al.* [28], who have investigated the binding of lysozyme to pyrene-labeled polyanions. Macroscopic phase separation is found to occur in these systems due to the association of the complexes of the lysozyme dimers with polymers. The *p*H at which the macroscopic phase separation begins to occur depends on the ionic strength, which implies that the bulk phase separation is controlled by electrostatic interaction.

The microscopic origin of the cloud-point transition is elusive. Different models have been proposed to explain the phenomenon of clouding in macromolecular solutions. Water-mediated intermicellar interaction modeled in the form of the Yukawa potential has been used to explain the lower consolute boundary in nonionic micellar solutions [29]. The sticky hard sphere potential and Baxter model [30] have been used to determine the phase diagram of nonionic surfactant solutions [31] and sterically stabilized colloidal silica dispersions [32]. The phase boundaries of charged colloidal dispersions have been described using a sticky hard sphere reference system with DLVO perturbation potential treated in random phase approximation [33,34]. These models assume that the interacting particles are spherical in structure as liquid state theories of phase separation are far more advanced for this case. Description of anisotropic particles of moderate ratios of length to diameter as effective spheres is considered as a reasonable approximation in these models.

Regular solution theory and lattice models are also used to describe the consolution curves [35]. However, these theories are thermodynamic in origin and not molecular. The approach which uses a lattice model in the mean-field approximation was extended by Flory and Huggins [36] to polymer solutions. A generalized Flory-Huggins theory for polydisperse polymer solutions has been developed by Koningsveld [19] and Solc [20]. The experimental consolution curves of several polymer solutions could be accounted for by this theory [19]. Flory-Huggins theory has been used to explain the lower consolution boundary of nonionic micellar solutions [37,38]. Treating the proteins unfolded by bound surfactant micelles as polymerlike objects, Guo and Chen [14] have applied the Flory-Huggins theory for polydisperse polymers to describe the cloud-point curve of BSA-SDS complexes in solution. We recapitulate this polymer phase-separation theory in the following.

If the interaction parameter χ ($\sim$const/T) is assumed to be independent of the volume fraction of polymers, the cloud-point curve equation for the Flory-Huggins system can be written in the form [20]

$$\frac{1}{2}K\sigma(1+\nu_0)+(\nu_0-1)-(\nu_{-1}-\mu_{-1}) + \left[\phi^{-1}-\frac{1}{2}(1+\nu_0)\right]\ln\left(\frac{1-\phi\nu_0}{1-\phi}\right)=0, \qquad (1)$$

where ϕ is the volume fraction of the polymer in solution, μ_k are the statistical moments of the normalized chain-length distribution $w(x)$ of the polymer under investigation, and ν_k are the statistical moments of the unnormalized distribution of the polymer contained in the incipient phase.

$$\mu_k=\int_0^\infty x^k w(x)dx \quad \text{and} \quad \nu_k=\int_0^\infty x^k w(x)\exp(K\sigma x)dx. \qquad (2)$$

The constant $K=1$ if $\phi<\phi_C$ and -1 if $\phi>\phi_C$, where ϕ_C is the critical volume fraction given by

$$\phi_C=(1+x_w x_z^{-1/2})^{-1}. \qquad (3)$$

x_w and x_z are, respectively, the weight average and z-average chain lengths of the polymer. Since $\mu_1=x_w$ and $\mu_2/\mu_1=x_z$,

$$\phi_C=(1+\mu_1^{3/2}\mu_2^{-1/2})^{-1}. \qquad (4)$$

The positive parameter σ is related to the interaction parameter χ through

$$2\chi\phi(\nu_0-1)=K\sigma+\ln\left[\frac{1-\phi}{1-\phi\nu_0}\right]. \qquad (5)$$

At the critical point,

$$\chi C = \tfrac{1}{2}(1+x_z^{1/2}x_w^{-1})(1+x_z^{-1/2})$$
$$= \tfrac{1}{2}(1+\mu_1^{-3/2}\mu_2^{1/2})(1+\mu_1^{1/2}\mu_2^{-1/2}). \quad (6)$$

Hence for a given normalized chain-length distribution $w(x)$ of the polymer under investigation, all the statistical moments μ_k and ν_k can be evaluated and using Eqs. (1)–(6) the cloud-point curve can be theoretically determined.

For polymers with exponential distribution [20],

$$w(x) = t^{u+1}\Gamma^{-1}(u+1)x^u \exp(-tx). \quad (7)$$

The moments of the polymer distribution are given by

$$\mu_k = \frac{\Gamma(u+k+1)}{\Gamma(u+1)} t^{-k} \quad (8)$$

and

$$\nu_k = \frac{\Gamma(u+k+1)}{\Gamma(u+1)} \frac{t^{u+1}}{(t-K\sigma)^{u+k+1}}, \quad (9)$$

with $\sigma < t$, since $K = \pm 1$.

Applying the above phase-separation theory to BSA-SDS complexes in solution, Guo and Chen [14] have assumed the effective chain-length distribution to be a Schulz distribution. In this case $w(x)$ is identical to Eq. (7) with $t=(u+1)/\overline{x}$, where u is an integer and $\mu_1 = \overline{x}$. The parameter u indicates the polydispersity of the sample; the smaller the value of u, the larger is the polydispersity. Drawing an analogy with the BSA-SDS system, we apply the polymer phase-separation theory to explain the cloud-point curve of lysozyme-SDS complexes in solution.

If the phase volumes of the phase-separated sample at a temperature very close to the cloud-point temperature are equal, then the sample can be considered to be at the critical concentration [14,39]. The lysozyme-SDS sample of 12 wt % at *p*H 10 (lysozyme:SDS=1:2 and [NaCl]=0.4*M*) was set at a temperature 1 °C below the cloud-point temperature and allowed to phase separate. The volumes of both phases were found to be almost equal. Hence 12 wt % was assumed to be the critical concentration. The critical volume fraction ϕ_C was calculated using the specific volumes of lysozyme (0.703 $cm^3\,g^{-1}$) and SDS (0.847 $cm^3\,g^{-1}$). Using the experimental data shown in Fig. 2, the cloud-point curve was recalculated in terms of T/T_C and ϕ, where T_C (K) is the cloud-point temperature at $\phi = \phi_C$.

From the experimental value of ϕ_C, for a given polydispersity parameter u, the average effective chain length $\mu_1 = \overline{x}$ can be obtained by solving Eq. (4) and hence all μ_k and ν_k can be computed. For every assigned ϕ, the interaction parameter χ can be solved from Eqs. (1) and (5) numerically. Since $\chi \sim \text{const}/T$, $\chi_C/\chi \sim T/T_C$. The experimental (T/T_C vs ϕ) and theoretical (χ_C/χ vs ϕ) cloud-point curves are shown in Fig. 6. It was found that only $u=3$ could fit the experimental data satisfactorily. The quality of the fit near the precipitation threshold, which is the maximum of the cloud-point curve, is not very good. $u=1$ gave a good fit near the precipitation threshold, but a very bad fit at lower volume fractions. The theoretical curve in Fig. 6 corresponds to the polydispersity index, $u=3$, and the average effective chain length $\mu_1 = 105$. The small-u value indicates that the lysozyme-SDS complexes are highly polydisperse.

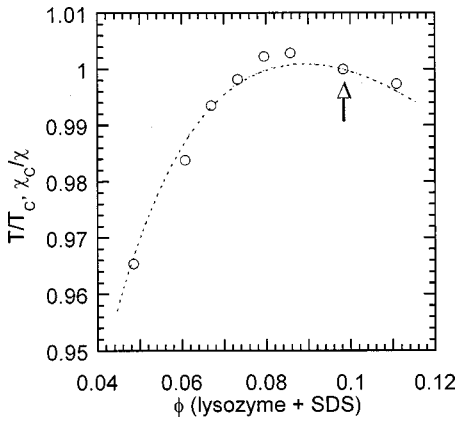

FIG. 6. Theoretical fit to the experimental data of the cloud-point curve in Fig. 2. The dotted line is the theoretical cloud-point curve ($\chi c/\chi$ vs ϕ) calculated using the polymer phase-separation model with polydispersity index $u=3$ and an average effective chain length $\mu_1 = 105$. Circle corresponds to *p*H=10.0 of Fig. 2. The experimental data were recalculated in terms of T/T_C and ϕ (refer text). The arrow indicates the critical point.

Though the polymer phase-separation theory reproduces the experimental cloud curve, the exact nature of the interparticle interaction force is difficult to assess. It could be the resultant of the repulsive Coulomb and attractive van der Waals and attractive (hydrophobic) solvation forces [40]. In the preceding paragraphs we have explained the variation in cloud-point temperature with *p*H, salt concentration, and relative lysozyme to SDS ratio in terms of the electrostatic interactions. However, the role played by other repulsive interactions such as hydration forces [40] cannot be ignored.

SUMMARY

The phenomenon of clouding and liquid-liquid phase separation in lysozyme-SDS complexes in solution has been investigated under different solution conditions by varying the *p*H, salt concentration, and the relative weight ratio of lysozyme to SDS. The cloud-point temperature is found to be very sensitive to these parameters. The cloud-point curve can be described by a generalized Flory-Huggins theory for polydisperse polymers. This suggests that the lysozyme-SDS complexes behave like flexible polymers due to the unfolding of the protein by the bound surfactant micelles. For the temperature, concentration, and *p*H ranges used in this study, the clouding phenomenon appears to be controlled by the electrostatic interaction between the lysozyme-SDS complexes. A decrease in the net charge on the complexes by (i) varying the *p*H of the solution, (ii) changing the relative lysozyme to SDS ratio, and (iii) electrostatic screening of the charge by salt ions present in the solution leads to a reduction in repulsive interaction energy which results in an increase in the cloud-point temperature. However, the electrostatic interaction alone cannot account for other observed

phenomena such as irreversible gel formation and precipitation at high protein plus surfactant concentration and high salt concentration. Since a large number of parameters are involved in deciding the solution conditions that are conducive to bringing forth the clouding, a quantitative description of the clouding phenomenon requires further investigations on the protein-surfactant interactions.

ACKNOWLEDGMENTS

We are grateful to Dr. C. Manohar, P. A. Hassan, B. S. Valaulikar, and Usha Mukundan for their help, encouragement, and discussions. This work was supported by the BRNS under Research Project No. 37/9/96-G of the Department of Atomic Energy, Government of India.

[1] C. Tanford, *The Hydrophobic Effect: Formation of Micelles and Biological Membranes*, 2nd ed. (Wiley Interscience, New York, 1980).
[2] K. P. Ananthapadmanabhan, in *Interactions of Surfactants with Polymers and Proteins*, edited by E. D. Goddard and K. P. Ananthapadmanabhan (CRC Press, London, 1993).
[3] X. H. Guo, N. M. Zhao, S. H. Chen, and J. Teixeira, Biopolymers **29**, 335 (1990).
[4] S. H. Chen and J. Teixeira, Phys. Rev. Lett. **57**, 2583 (1986).
[5] S. H. Chen, E. Y. Sheu, J. Kalus, and H. Hoffmann, J. Appl. Crystallogr. **21**, 751 (1988).
[6] M. N. Jones and P. Manely, J. Chem. Soc., Faraday Trans. 1 **75**, 1736 (1979); **76**, 654 (1980).
[7] M. N. Jones, G. Preito, J. M. del Rio, and F. Sarmiento, J. Chem. Soc., Faraday Trans. **91**, 2805 (1995).
[8] N. J. Turro, X. G. Lei, K. P. Ananthapadmanabhan, and M. Aronson, Langmuir **11**, 2525 (1995).
[9] K. Fukushima, Y. Murata, G. Sugihara, and M. Tanaka, Bull. Chem. Soc. Jpn. **55**, 1376 (1982).
[10] K. Fukushima, Y. Murata, N. Nishikido, G. Sugihara, and M. Tanaka, Bull. Chem. Soc. Jpn. **54**, 3122 (1981).
[11] J. Oakes, J. Chem. Soc., Faraday Trans. 1 **70**, 2200 (1974).
[12] A. K. Moren and A. Khan, Langmuir **11**, 3636 (1995).
[13] M. N. Jones, Biochem. J. **151**, 109 (1975).
[14] X. H. Guo and S. H. Chen, Phys. Rev. Lett. **64**, 1979 (1990).
[15] C. Tanford and R. Roxby, Biochemistry **11**, 2192 (1972).
[16] W. J. Fredericks, M. C. Hammonds, S. B. Howard, and F. Rosenberg, J. Cryst. Growth **141**, 183 (1994).
[17] M. L. Broide, T. M. Tominc, and M. D. Saxowsky, Phys. Rev. E **53**, 6325 (1996).
[18] E. J. W. Verwey and J. Th. G. Overbeek, *Theory of the Stability of Lyophobic Colloids* (Elsevier, Amsterdam, 1948).
[19] R. Koningsveld, Adv. Colloid Interface Sci. **2**, 151 (1968).
[20] K. Solc, J. Polym. Sci., Phys. Ed. **12**, 555 (1974); **12**, 1865 (1974).
[21] A. J. Sophianopoulos and K. E. van Holde, J. Biol. Chem. **239**, 2156 (1964).
[22] O. H. Lowry, N. J. Rosebrough, A. L. Farr, and R. J. Randall, J. Biol. Chem. **193**, 265 (1951).
[23] A. A. Green, J. Am. Chem. Soc. **55**, 2331 (1933).
[24] N. A. Mazer, G. B. Benedek, and M. C. Carey, J. Phys. Chem. **80**, 1075 (1976).
[25] J. A. Reynolds and C. Tanford, Proc. Natl. Acad. Sci. USA **66**, 1002 (1970).
[26] D. Bendedouch, S. H. Chen, and W. C. Koehler, J. Phys. Chem. **87**, 2621 (1983).
[27] T. Sasaki, M. Hattori, J. Sasaki, and K. Nukina, Bull. Chem. Soc. Jpn. **48**, 1397 (1975).
[28] T. Sato, K. W. Mattison, P. L. Dubin, M. Kamachi, and Y. Morishima, Langmuir **14**, 5430 (1998).
[29] J. B. Hayter and M. Zulauf, Colloid Polym. Sci. **260**, 1023 (1982).
[30] R. J. Baxter, J. Chem. Phys. **49**, 2770 (1968).
[31] S. V. G. Menon, V. K. Kelkar, and C. Manohar, Phys. Rev. A **43**, 1130 (1991).
[32] M. H. G. M. Penders, A. Vrij, and R. van der Haegen, J. Colloid Interface Sci. **144**, 86 (1991).
[33] M. J. Grimson, I. L. McLaughlin and M. Silbert, J. Phys.: Condens. Matter **3**, 7995 (1991).
[34] C. Manohar and V. K. Kelkar, Langmuir **8**, 18 (1992).
[35] T. L. Hill, *An Introduction to Statistical Thermodynamics* (Addison-Wesley, Reading, MA, 1960).
[36] P. J. Flory, *Principles of Polymer Chemistry* (Cornell University Press, Ithaca, NY, 1953), Chaps. 12 and 13.
[37] V. Degiorgio, in *Physics of Amphiphiles: Micelles, Vesicles and Microemulsions*, edited by V. Degiorgio and M. Corti (North-Holland, Amsterdam, 1985), p. 303.
[38] R. Kjellander, J. Chem. Soc., Faraday Trans. 2 **78**, 2025 (1982).
[39] R. Koningsveld and A. J. Staverman, J. Polym. Sci. Part A-2 **6**, 325 (1968).
[40] J. N. Israelachvili, *Intermolecular and Surface Forces* (Academic, San Diego, 1985).